

Performance Parameters and Frequency Response of CMUTs in Transmit, Receive, and Pulse-Echo Operation

Ira Wygant
Swift Sensing
Palo Alto, USA

ira.wygant@swiftsensing.com
https://orcid.org/0000-0002-0178-6813

Butrus T. Khuri-Yakub
Department of Electrical Engineering
Stanford University
Stanford, USA
pierrek@stanford.edu

Mario Kupnik
Technische Universität Darmstadt
Darmstadt, Germany
mario.kupnik@tu-darmstadt.de

Abstract— Models of electrostatic transducers that assume a constant shape function for the plate’s deflection facilitate derivation of closed-form design expressions. This work analyses the static and frequency-response characteristics of capacitive micromachined ultrasonic transducers (CMUTs) using a shape-function based model. This analysis shows that across all CMUT designs of a given plate shape, the CMUT’s static parameters vary with bias voltage in the same manner. Normalizing bias voltage by pull-in voltage and plate deflection by gap height enables this result. The static parameters examined are plate deflection, capacitance, transformer ratio, spring softening, and coupling coefficient. As shown here, assuming a basic second-order model of the CMUT, these static parameters along with plate resonance frequency and quality factor describe a CMUT’s frequency response. This work specifically examines ideal parallel-plate and clamped circular plate CMUTs, but it extends to other plate shapes with substitution of different expressions for capacitance as a function of plate deflection.

Keywords— *Capacitive micromachined ultrasonic transducer (CMUT), equivalent circuits, microelectromechanical devices, sensor device modeling.*

I. INTRODUCTION

The lumped-element electromechanical model shown in Fig. 1(a) describes the CMUT’s operation for a single resonance frequency. For given CMUT dimensions and material properties, one approach to calculating parameters for this model is to assume a constant shape function for the CMUT plate [1, 2]. This shape function describes the plate’s shape relative to a single lumped-element deflection parameter.

The shape-function approach has useful properties: it results in analytical expressions for the lumped-element model in terms of CMUT geometry; it applies to various plate shapes, e.g., circular [1, 3, 4] and square [3, 5]; and it enables fast simulations that agree with finite-element modeling and experiments.

This work develops new analytical expressions for CMUT performance using shape-function-based CMUT models. These expressions describe performance across all CMUT designs based on just a few design parameters: plate resonance frequency, quality factor, and bias voltage normalized to pull-in

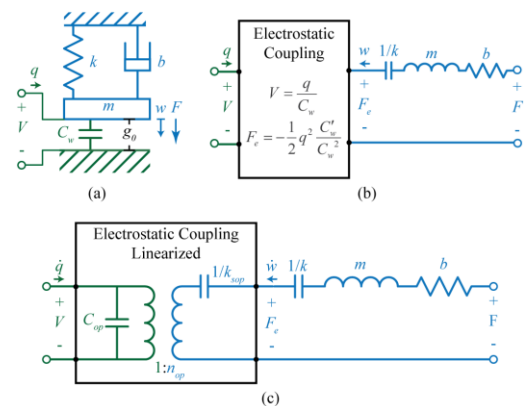


Fig. 1. Lumped-element model of an electrostatic transducer used to model the CMUT. (a) Electromechanical system representation with spring constant k , mass m , damping factor b , capacitance function C_w , and initial gap height g_0 . (b) Circuit representation with nonlinear electrostatic coupling equations. (c) Linearized equivalent circuit.

voltage. The outcome is a set of simple design expressions that yield greater insight into CMUT performance than can be achieved simply from running batches of simulations.

The second-order model assumed here enables this insight and results in simple design expressions. It is also an accurate model for a CMUT operating at dc and in air. However, it does not accurately predict the wideband response of CMUTs operating in liquids or solids because it is missing effects such as complex radiation impedance and higher-order resonances. Nonetheless, this work still yields useful insights for design of those devices.

Analysis for this work begins in Section II with a derivation of the CMUT’s equivalent circuit. Typical equivalent circuit derivations assume capacitance varies with deflection as a parallel-plate capacitor. In contrast, this work’s derivation uses a generic capacitance function, C_w , so that the resulting expressions apply to any plate shape.

Subsequent sections analyze the CMUT’s pull-in and linear equivalent circuit parameters in terms of C_w . Normalizing

deflection by gap height and bias voltage by pull-in voltage simplifies this analysis. By substituting appropriate expressions for C_w , Section VI examines the static operating-point parameters of parallel-plate and clamped circular plate CMUTs. Finally, Section VII studies the CMUT's transmit and receive frequency responses in terms of the CMUT's static operating-point parameters, plate resonance frequency, and quality factor.

II. LUMPED-ELEMENT TRANSDUCER MODEL

Using the direct electromechanical analogy, Fig. 1(b) gives a circuit representation of the system in Fig. 1(a) [6]. In this circuit, a two-port component represents the transducer's nonlinear electrostatic coupling equations that relate voltage V and force F_e to charge q and displacement w .

The electrostatic coupling equations derive from conservation of energy [6, 7]. Applying conservation of energy to the electrostatic coupling block in Fig. 1(b), dictates that the sum of electrical and mechanical energy flowing into the coupling component must equal the change in its stored energy, U , i.e.,

$$V\delta q + F_e\delta w = \frac{\partial U}{\partial q}\delta q + \frac{\partial U}{\partial w}\delta w \quad (1)$$

Substituting the stored energy for an electrostatic transducer, $q^2/(2C_w)$, into (1) and solving for all changes in charge δq and displacement δw yields equations for force

$$F_e(q, w) = -\frac{1}{2} \frac{q^2 C'_w}{C_w^2} \quad (2)$$

and voltage

$$V(q, w) = \frac{q}{C_w}, \quad (3)$$

where C'_w is the derivative of capacitance with respect to deflection. Equations (2) and (3) are the electrostatic coupling equations. Combined with the circuit components in Fig. 1(b), they comprise a nonlinear electromechanical model of the CMUT.

III. STATIC PLATE DEFLECTION AND PULL-IN

At rest, the sum of the forces on the plate equals zero. For bias voltage V_b , bias force F_b , and substitution of $V_b C_w$ for q , the sum of the forces on the plate equals

$$F_{sum}(w) = F_e + kw - F_b = -\frac{1}{2} C'_w V_b^2 + kw - F_b. \quad (4)$$

Setting (4) equal to zero and solving for w yields the plate's static deflection for a given bias voltage and force.

Plate deflection increases with increasing bias voltage until pull-in, at which point the plate snaps to the cavity bottom. For deflection equal to the pull-in deflection w_{pi} , F_{sum} and its derivative with respect to w are both zero. These conditions imply that the plate is stable but will become unstable for larger

deflections [8]. Applying these conditions to (4) and eliminating the bias voltage yields

$$kC'_{w_{pi}} + (F_b - kw_{pi})C''_{w_{pi}} = 0, \quad (5)$$

where C'' is the second derivative of capacitance with respect to deflection. Solving (5) for w_{pi} yields the pull-in deflection. In terms of w_{pi} , the pull-in voltage equals

$$V_{pi} = \sqrt{\frac{2k}{C''_{w_{pi}}}}. \quad (6)$$

IV. LINEARIZED EQUIVALENT CIRCUIT

Expressing the electrostatic coupling equations as a linear circuit requires linearizing them about an operating point determined by the bias conditions [6, 8]. In matrix form, the linearized equations are

$$\begin{bmatrix} \delta V \\ \delta F_e \end{bmatrix} = \mathbf{B} \begin{bmatrix} \delta q \\ \delta w \end{bmatrix} = \begin{bmatrix} \frac{\partial V}{\partial q} & \frac{\partial V}{\partial w} \\ \frac{\partial F_e}{\partial q} & \frac{\partial F_e}{\partial w} \end{bmatrix} \begin{bmatrix} \delta q \\ \delta w \end{bmatrix} \\ = \frac{1}{s} \begin{bmatrix} \frac{1}{C_w} & -\frac{V_b C'_w}{C_w} \\ -\frac{V_b C'_w}{C_w} & \frac{V_b^2 C''_w}{C_w} - \frac{1}{2} V_b^2 C''_w \end{bmatrix} \begin{bmatrix} \delta q \\ \delta w \end{bmatrix}, \quad (7)$$

where the Laplace transform allows substitution of charge and displacement for current \dot{q} and velocity \dot{w} . Equating matrix \mathbf{B} in (7) with the impedance parameters for the equivalent circuit in Fig. 1(c) yields

$$C_{op} = C_{wop}, \quad (8)$$

$$n_{op} = -V_b C'_w, \quad (9)$$

and

$$k_{sop} = -\frac{1}{2} V_b^2 C''_w, \quad (10)$$

where w_{op} is the static plate deflection for the given bias conditions. Note that n_{op} is negative due to the sign convention adopted for w in Fig. 1(a) and Fig. 1(b).

V. NORMALIZING DEFLECTION BY GAP AND BIAS VOLTAGE BY PULL-IN VOLTAGE

Normalizing the deflection by the gap, $w_n = w/g_0$, and the bias voltage by the pull-in voltage, $V_n = V_b/V_{pi}$, simplifies some of the previous expressions.

First, consider the integral for computing the transducer's capacitance,

$$C = \int_A \frac{\epsilon_0}{g_0 - w S_{x,y}} dx dy = \frac{\epsilon_0 A}{g_0} \int_A \frac{1}{1 - w_n S_{x,y}} dx dy = \frac{\epsilon_0 A}{g_0} C_n, \quad (11)$$

where A is the transducer's area and S is the plate's shape function. From (11), the transducer's capacitance equals the product of its capacitance with zero deflection and a normalized capacitance C_n , which, for a given shape function, is just a function of w_n .

In terms of w_n and V_n spring softening equals

$$k_n = \frac{k_s + k}{k} = 1 - \frac{V_n^2 C_n''}{C_{npi}''}, \quad (12)$$

where C_n'' and C_{npi}'' are the second derivatives of C_n with respect to w_n for w_n at the operating point and pull-in point, respectively.

In terms of the transducer's equivalent circuit, the electromechanical coupling factor equals

$$k^2 = \frac{1}{k_n k \frac{C_w}{n^2} + 1} = \frac{1}{\frac{C_n (C_{npi}'' - V_n^2 C_n'')}{2V_n^2 C_n'^2} + 1}. \quad (13)$$

Significantly, expressions (12) and (13) depend only on w_n and V_n . In other words, across all CMUT designs, spring softening and coupling coefficient depend only on normalized deflection and bias voltage.

Often, the bias force F_b is negligible. For example, transducers designed for liquids and solids have mechanical impedances commensurate with those mediums, and thus, they have stiff plates relative to atmospheric pressure.

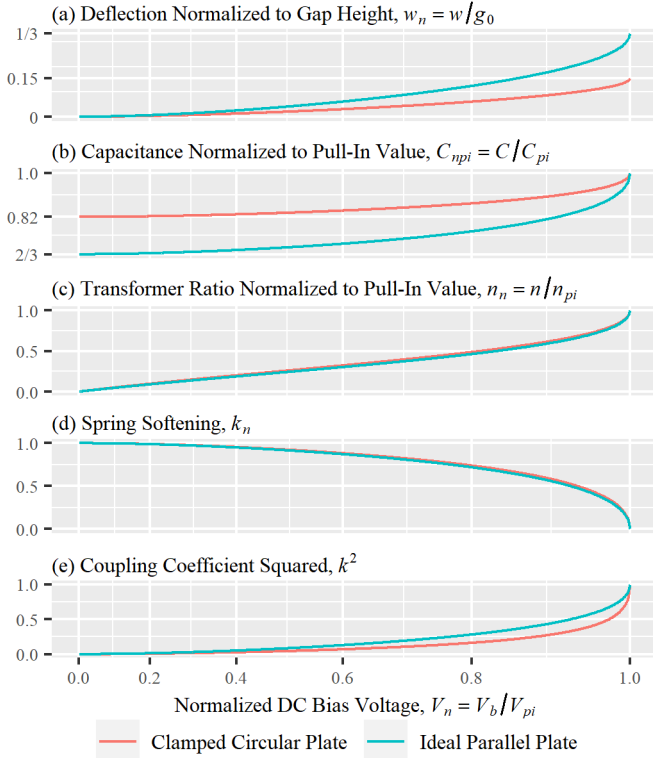


Fig. 2. Normalized parameter curves for clamped circular-plate and ideal parallel-plate transducers as a function of bias voltage normalized to pull-in voltage.

If the bias force is negligible, then w_n depends only on V_n . Neglecting bias force and setting (4) equal to zero yields

$$w_n - \frac{V_n^2 C_n'}{C_{npi}''} = 0. \quad (14)$$

Solving (14) for w_n , yields w_n in terms of V_n .

Neglecting bias force in (5) produces

$$C_{npi}' - w_{npi} C_{npi}'' = 0. \quad (15)$$

Solving (15) yields the normalized pull-in deflection, w_{npi} , which is a constant.

VI. THE IDEAL PARALLEL-PLATE AND CLAMPED CIRCULAR PLATE TRANSDUCERS

Table I summarizes the shape functions and capacitance functions for the ideal parallel-plate and clamped circular plate transducers. The shape function for the clamped circular plate is in terms of plate radius a and polar coordinate r [1].

Combining these capacitance functions with expressions from the previous section produces the operating-point curves in Fig. 2 and pull-in parameters in Table II. Note the coupling coefficient curve in Fig. 2(e) matches the results obtained with finite-element modeling and experiments in [9].

TABLE I
CAPACITANCE AND DERIVATIVES WITH RESPECT TO DEFLECTION

Param.	Parallel Plate	Clamped Circular Plate
S	1	$3(1 - \frac{r^2}{a^2})^2$
C_n	$\frac{1}{1 - w_n}$	$\frac{\tanh^{-1}(\sqrt{3w_n})}{\sqrt{3w_n}}$
$C_n' = \frac{dC_n}{dw_n}$	$\frac{1}{(1 - w_n)^2}$	$\frac{1}{2w_n - 6w_n^2} - \frac{\tanh^{-1}(\sqrt{3w_n})}{2\sqrt{3w_n^{3/2}}}$
$C_n'' = \frac{d^2C_n}{dw_n^2}$	$\frac{2}{(1 - w_n)^3}$	$\frac{\sqrt{3} \tanh^{-1}(\sqrt{3w_n})}{4w_n^{5/2}} - \frac{3(1 - 5w_n)}{4(1 - 3w_n)^2 w_n^2}$

TABLE II
TRANSDUCER PARAMETERS AT PULL-IN

Param.	Parallel Plate	Clamped Circular Plate
V_{pi}	$\sqrt{\frac{8}{27} \frac{g_0^3 k}{\epsilon_0 A}}$	$\sqrt{0.148 \frac{g_0^3 k}{\epsilon_0 A}}$
w_{npi}	1/3	0.154
C_{pi}	$\frac{3}{2} \frac{\epsilon_0 A}{g_0}$	$\frac{1.22 \epsilon_0 A}{g_0}$
n_{pi}	$\sqrt{\frac{3}{2} \frac{\epsilon_0 A k}{g_0}}$	$0.802 \sqrt{\frac{\epsilon_0 A k_0}{g_0}}$

TABLE III
TRANSMIT AND RECEIVE TRANSFER FUNCTIONS

Param. ^a	Transmit H_{TX}	Receive H_{RX}
$ H(s) $	$\frac{n \omega_0}{A Q} \frac{s}{s^2 + \frac{\omega_0 s}{Q} + k_n \omega_0^2}$	$\frac{A k^2 k_n \omega_0^2}{n (1-k^2)} \frac{1}{s^2 + \frac{\omega_0 s}{Q} + \frac{k_n \omega_0^2}{1-k^2}}$
s_p	$-\frac{\omega_0}{2Q} \pm j\omega_0 \sqrt{k_n - \frac{1}{4Q^2}}$	$-\frac{\omega_0}{2Q} \pm j\omega_0 \sqrt{\frac{k_n}{1-k^2} - \frac{1}{4Q^2}}$
$ H(s) _{\omega \rightarrow 0}$	0	$\frac{A}{n} k^2$
ω_{max}	$\sqrt{k_n} \omega_0$	$\omega_0 \sqrt{\frac{k_n}{1-k^2} - \frac{1}{2Q^2}}$
$ H(j\omega_{max}) $	$\frac{n}{A}$	$\frac{A}{n} \frac{2k^2 Q^2 k_n}{\sqrt{(1-k^2)(4Q^2 k_n + k^2 - 1)}}$
ω_{-3dB}	$\frac{\omega_0}{2Q} (\sqrt{1+4k_n Q^2} \pm 1)$	$\omega_0 \sqrt{\frac{k_n}{1-k^2} - \frac{1}{2Q^2}} \pm \sqrt{\frac{1}{Q^2} \frac{k_n}{1-k^2} - \frac{1}{4Q^4}}$
FBW	$\frac{1}{Q}$	$\approx \frac{1}{Q} \sqrt{\frac{1-k^2}{k_n}}$

^a s_p : pole frequencies, ω_{max} : frequency for maximum response, FBW: fractional bandwidth

VII. FREQUENCY RESPONSE

In terms of the equivalent circuit in Fig. 1(c), the transducer's transmit transfer function, H_{TX} , equals the ratio of the pressure (force divided by area) across b to input voltage. Its open-circuit receive transfer function, H_{RX} , equals the ratio of the voltage across C_{op} to input pressure. Based on analysis of Fig. 1(c), Table III describes H_{TX} and H_{RX} in terms of A , n , k^2 , k_n , plate resonance frequency ω_0 ,

$$\omega_0 = \sqrt{\frac{k}{m}} \quad (16)$$

and quality factor Q ,

$$Q = \frac{\sqrt{mk}}{b}. \quad (17)$$

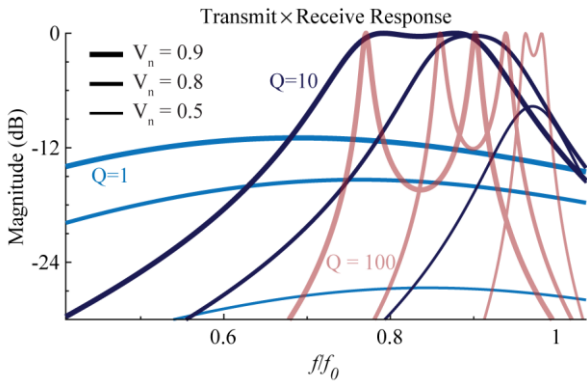


Fig. 3. Magnitude of the transmit-receive response H_{TXRX} for a clamped circular-plate transducer. For Q equal one, the response has wide bandwidth but relatively low sensitivity. For higher Q , sensitivity is higher and saturates at 0 dB (1 V/V). For higher Q and V_n , separate peaks from the transmit and receive responses are distinguishable.

Fig. 3 plots the transmit-receive frequency response, $H_{TX} \times H_{RX}$, for several values of Q and V_n . These plots show that sensitivity and bandwidth increase with increasing bias voltage until sensitivity saturates at 1 V/V. After saturation, the transducer's bandwidth continues growing due to increased separation between the poles of H_{TX} and H_{RX} .

VIII. CONCLUSION

This work shows that resonance frequency, quality factor, and bias voltage normalized to pull-in voltage are critical determinants of CMUT performance. Describing a CMUT in terms of these parameters facilitates accurate transducer analysis and design. Plots of static parameters versus normalized bias voltage highlight the importance of biasing the CMUT close to its pull-in voltage. These parameter curves also help compare plate shapes and interpret dc finite-element model and experimental results.

Although the assumption of a constant radiation impedance and a single resonance frequency is an oversimplification for some devices, the frequency-response analysis presented here helps design of those devices. The results show, across all CMUT designs, how the transmit and receive frequency responses evolve with increasing bias voltage. And they show the importance of quality factor and coupling coefficient to bandwidth and sensitivity.

REFERENCES

- [1] I. O. Wygant, M. Kupnik, and B. T. Khuri-Yakub, "An Analytical Model for Capacitive Pressure Transducers With Circular Geometry," *Journal of Microelectromechanical Systems*, vol. 27, no. 3, pp. 448-456, 2018.
- [2] A. Lohfink and P. Ecardt, "Linear and nonlinear equivalent circuit modeling of CMUTs," *IEEE Transactions on Ultrasonics, Ferroelectrics, and Frequency Control*, vol. 52, no. 12, pp. 2163-2172, 2005.
- [3] M. F. I. Cour, T. L. Christiansen, J. A. Jensen, and E. V. Thomsen, "Electrostatic and small-signal analysis of CMUTs with circular and square anisotropic plates," *IEEE Transactions on Ultrasonics, Ferroelectrics, and Frequency Control*, vol. 62, no. 8, pp. 1563-1579, 2015.
- [4] H. Koymen, A. Atalar, E. Aydogdu, C. Kocabas, H. K. Oguz, S. Olcum, A. Ozgurluk, and A. Unlugedik, "An improved lumped element nonlinear circuit model for a circular CMUT cell," *IEEE Transactions on Ultrasonics, Ferroelectrics, and Frequency Control*, vol. 59, no. 8, pp. 1791-1799, 2012.
- [5] M. Maadi and R. J. Zemp, "A Nonlinear Lumped Equivalent Circuit Model for a Single Un-Collapsed Square CMUT Cell," *IEEE Transactions on Ultrasonics, Ferroelectrics, and Frequency Control*, pp. 1-1, 2019.
- [6] H. A. C. Tilmans, "Equivalent circuit representation of electromechanical transducers: I. Lumped-parameter systems," *Journal of Micromechanics and Microengineering*, vol. 6, no. 1, pp. 157-176, 1996/03/01, 1996.
- [7] H. H. Woodson and J. R. Melcher, *Electromechanical Dynamics*, New York: John Wiley & Sons, 1968.
- [8] S. D. Senturia, *Microsystem Design*, New York: Kluwer Academic Publishers, 2001.
- [9] G. G. Yaralioglu, A. S. Ergun, B. Bayram, E. Haeggstrom, and B. T. Khuri-Yakub, "Calculation and measurement of electromechanical coupling coefficient of capacitive micromachined ultrasonic transducers," *IEEE Transactions on Ultrasonics, Ferroelectrics, and Frequency Control*, vol. 50, no. 4, pp. 449-456, 2003.